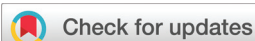


PAPER

Cite this: *Food Funct.*, 2020, **11**, 1547

A jaboticaba extract prevents prostatic damage associated with aging and high-fat diet intake†

C. A. Lamas,^a L. A. Kido,^{a,b} F. Montico,^a C. B. Collares-Buzato,^c
M. R. Maróstica, Junior^b and V. H. A. Cagnon *^a

Aging and overweight are involved in prostatic lesion development, due to their association with cell proliferation, hormonal imbalance and angiogenesis. The jaboticaba fruit is rich in bioactive compounds, showing potential chemopreventive action such as the capacity to modulate hormones and angiogenesis hallmarks. This study aimed to evaluate the jaboticaba extract (PJE) effect on the prostate morphology and on molecules related to hormone signaling and angiogenesis, during aging and/or high-fat diet (HFD) intake. Seventy FVB mice were distributed into experimental groups: YG group (young: 3 month old mice), AG group (aged: 11 month old mice), HfAG group (aged + HFD), JAGI group (aged + 2.9 g kg⁻¹ PJE), JAGII group (aged + 5.8 g kg⁻¹ PJE), HfJAGI group (aged + HFD + 2.9 g kg⁻¹ PJE) and HfJAGII group (aged + HFD + 5.8 g kg⁻¹ PJE). The ventral prostate was collected for morphological, immunohistochemistry and western-blotting analysis after 60 days of treatment. All PJE treatments promoted hormonal signaling balance and inhibited angiogenesis in the prostates of aged or HFD-fed aged mice, leading to the maintenance of healthy prostate morphology. A high dose of the PJE (JAGII and HfJAGII groups) led to the best capacity to reduce AR (58.40% and 74.42%; $p = 0.0240$ and $p = 0.0023$), ER α (30.29% and 45.12%; $p = 0.0004$ and $p < 0.0001$), aromatase (39.54% and 55.94%; $p = 0.0038$ and $p = 0.0020$), and VEGF (50.81% and 67.68%; $p < 0.0001$) and increase endostatin immunoeexpression. Moreover, HFD intake intensified the hormonal and angiogenic alterations in the aged mouse prostates, contributing to the increase in premalignant lesion incidence. The PJE exerted a dose-dependent positive effect on aged or HFD-fed aged mouse prostates, contributing to the gland microenvironment recovery, mainly due to the hormonal and angiogenic balance. Therefore, we suggest that the PJE can be a potential candidate for prostatic lesion prevention.

Received 7th November 2019,
Accepted 22nd December 2019

DOI: 10.1039/c9fo02621e

rsc.li/food-function

Introduction

Aging is an important risk factor for the development of prostate disorders, including prostate adenocarcinoma, the second most frequent type of cancer among men in the world.^{1,2} It is known that there is an increase in the incidence and mortality due to prostate cancer in men over the age of fifty, which makes the aging population a worldwide concern.^{1,2} Also, studies show that hormonal imbalance

occurs during late life, which is characterized by a progressive decrease of androgen associated with high estrogen levels.^{3–5} The stimulation of aromatase during this period of life contributes to increasing androgen conversion into estrogen, exacerbating the hormonal alterations, directly related to the development of prostate premalignant lesions.^{6–8}

Angiogenesis plays an essential role in prostate lesion dynamics.^{9–12} This process is natural in the organism, leading to the formation of new blood vessels.¹³ The imbalance between angiogenic inducer and inhibitor factors in the prostate stimulates this process, leading to nutrient and oxygen supply for cell proliferation and cancer progression in this gland.^{10,13} In addition, there are different angiogenesis molecular markers related to the stimulus or suppression of this process such as vascular endothelial growth factor (VEGF) and endostatin, respectively.^{12,13} VEGF promotes the proliferation, differentiation and migration of endothelial cells.^{14,15} On the other hand, endostatin has the opposite action, blocking the

^aDepartment of Structural and Functional Biology, Institute of Biology, University of Campinas, Bertrand Russel Av, Campinas, São Paulo, 13083-865, Brazil.

E-mail: quitete@unicamp.br

^bDepartment of Food and Nutrition, School of Food Engineering, University of Campinas, 80 Monteiro Lobato St, Campinas, São Paulo, 13083-852, Brazil

^cDepartment of Biochemistry and Tissue Biology, Biology Institute, University of Campinas, 255 Monteiro Lobato St, Campinas, São Paulo, 13083-970, Brazil

†Electronic supplementary information (ESI) available. See DOI: 10.1039/c9fo02621e

proliferation and migration of endothelial cells, besides inducing their apoptosis.^{15,16}

It is known that the incidence of overweight has increased in the aging population in the last few years.¹⁷ Several studies have demonstrated the relationship between obesity or overweight and prostatic alterations.^{18,19} Obesity is characterized by the accumulation of adipose tissue, and both the amount and quality of fat intake are important factors for its development.^{19,20} According to previous studies, high-fat diet (HFD) intake during aging promoted overweight in mice²¹ besides being correlated to prostate cancer onset.²² Furthermore, studies have shown that obesity-associated dysfunctions, such as inflammation, hyperinsulinemia and dyslipidemia, are involved in cell proliferation and tissue remodeling in the prostate.^{23–26}

Different authors have pointed out that weight gain directly influences the homeostasis of the sex hormone, which is correlated with changes in the serum level of testosterone and estrogen, leading to an imbalance in the interactions between the prostatic epithelial and stromal cells.^{19,20} Moreover, the disturbance of prostatic homeostasis, triggered by HFD intake, stimulates other processes such as cell migration and angiogenesis, increasing vascular permeability and lesion invasiveness.^{19,27}

Taking into consideration all the above information, different natural compounds have been studied to prevent or delay prostatic alterations.²⁸ Harper *et al.*²⁸ confirmed that epigallocatechin-3-gallate, a natural polyphenol, delayed prostate cancer development in a transgenic animal model. Quercetin, a natural flavonoid, regulated cell proliferation, anti-apoptotic markers and androgen receptor (AR) levels in an *in vivo* prostate cancer model.²⁹ In addition, green tea in association with quercetin reduced tumor growth and the VEGF level in xenograft prostate tumors.³⁰

Similarly, several types of fruits have been highlighted as being natural promising alternatives to protect different tissues and to prevent metabolic damage, due to their high bioactive compound content, and they have shown antioxidant and anti-inflammatory properties.^{31–33} A recent study by our research group demonstrated the anti-inflammatory, antioxidant and anti-obesity effects of the jaboticaba peel extract.²¹ Jaboticaba is a Brazilian fruit, which is round, has a purple peel, and has a white and sweet pulp with about four seeds inside.³⁴ Furthermore, a high content of polyphenols that show therapeutic functions was found in this fruit peel, such as anthocyanins, ellagic acid, quercetin, gallic acid and epicatechin.^{21,35}

Thus, considering the beneficial effects of the jaboticaba peel and the high incidence of damage in the prostate due to aging and overweight, we aimed to evaluate the prostate micro-environment after treatment with jaboticaba peel extract (PJE) in high-fat-fed aging mice. This study focused on morphological features, hormonal parameters and angiogenesis considering the importance of these processes in malignant and pre-malignant lesion development in the prostate during aging and high-fat diet intake.

Materials and methods

Jaboticaba peel extract (PJE)

The preparation method of the PJE has been patented and is described by Lamas *et al.*²¹ and Maróstica Junior *et al.*³⁶ In brief, freeze-dried jaboticaba peel (*Myrciaria cauliflora* (Vell.) Berg) was mixed with an ethanol solution, which was later removed from the preparation. The detailed characterization of the PJE, used in the study herein, including the nature of its bioactive compounds and its antioxidant activity *in vitro*, was described by Lamas *et al.*²¹

The doses of the PJE used in the present study were based on the previous data reported by our group.²¹ The high-performance liquid chromatography analysis of the dried extract showed that it contained 13.28 mg g⁻¹ cyanidin-3-*O*-glucoside, 1.428 mg g⁻¹ delphinidin-3-*O*-glucoside, 0.196 mg g⁻¹ ellagic acid, 0.02 mg g⁻¹ rutin and 0.017 mg g⁻¹ gallic acid.^{21,37} We also observed the presence of the following bioactive compounds in the PJE based on the fragmentation pattern of the analytical standard: HHDP-galloylglucose, bis-HHDP-glucose (casuariin), bis-HHDP-glucose isomer (pedunculagin), HHDP-galloylglucose isomer, (-)-epicatechin, galloyl-bis-HHDP-glucose (casuarinin), galloyl-bis-HHDP-glucose (casuarictin), HHDP-digalloylglucose (tellimagrandin I), kaempferol hexoside, chlorogenic acid, HHDP-trigalloylglucose (tellimagrandin II), pentagalloyl hexose, myricetin-rhamnoside, quercetin-3-rhamnoside (quercitrin), quercetin and naringenin.²¹ Based on these results, the experimental mice ingested the following daily quantities of these compounds according to the doses administered: 2.9 g kg⁻¹ PJE dose (4.65 mg cyanidin-3-*O*-glucoside, 0.5 mg delphinidin-3-*O*-glucoside, 0.07 mg ellagic acid, 0.007 mg rutin and 0.006 mg gallic acid) and 5.8 g kg⁻¹ PJE dose (9.3 mg of cyanidin-3-*O*-glucoside, 1 mg delphinidin-3-*O*-glucoside, 0.14 mg ellagic acid, 0.014 mg rutin and 0.012 mg gallic acid).

Animals and experimental design

Seventy male FVB mice were provided by the Multidisciplinary Center for Biological Investigation on Laboratory Animal Science of the University of Campinas. This research was approved by the Committee for Ethics in Animal Research of the University of Campinas (protocol no. 3421-1).

The mice were randomly divided into seven experimental groups ($n = 10$): the YG group: 3 month old mice treated with water (PJE vehicle) daily by gavage and a standard diet (Nuvital CR1, Colombo, Paraná, Brazil/composition: 22 g% protein; 53 g% carbohydrate; 4.5 g% lipid and 2.9 kcal g⁻¹). The AG group: 11 month old mice receiving the same treatment as the YG group. The HfAG group: 11 month old mice treated with water (PJE vehicle) daily by gavage and a HFD (composition: 20 g% protein; 50 g% carbohydrate; 21 g% lipid and 4.5 kcal g⁻¹). The JAGI group: 11 month old mice treated with the PJE (2.9 g PJE per kg body weight) daily by gavage and a standard diet. The JAGII group: 11 month old mice treated with the PJE (5.8 g PJE per kg body weight) daily by gavage and a standard diet. The HfJAGI group: 11 month old mice treated with the PJE (2.9 g PJE per kg body weight) daily by gavage and

a HFD. The HfJAGII group: 11 month old mice treated with the PJE (5.8 g PJE per kg body weight) daily by gavage and a HFD.

The animals were kept individually in cages, under controlled lighting conditions (12 hour light–dark cycle), with food and drinking water *ad libitum*. All the mice were treated for 60 days. At the end of the experimental protocol, the animals were weighed on a semi-analytical scale (Marte AS 5500, São Paulo, Brazil), anesthetized with xylazine hydrochloride (5 mg kg⁻¹ i.m.; König, Sao Paulo, Brazil) and ketamine hydrochloride (60 mg kg⁻¹ i.m.; Fort Dodge, Iowa, USA). The mice were euthanized by increasing the anesthetic level and ventral prostate samples were collected.

Morphological analysis

The ventral prostate samples from five mice per group were fixed in Bouin's solution for 24 hours. The samples were rinsed with ethanol (70%), dehydrated, diaphanized and embedded in plastic polymers (Paraplast Plus, St Louis, MO, USA). The prostate samples were sectioned into 5 µm thick slices using a micrometer (Hyrax M60, Zeiss, Germany). The slides were stained with Masson's Trichrome (Luz & Zancheta Neto, 2002) and 10 random images (400× magnification) per animal were captured using NIS-Elements software and a Nikon Eclipse E-400 microscope (Nikon, Tokyo, Japan). Then, using the Image Pro-Plus software, a grid containing 432 intersections was projected over these images. A total of 4320 points were evaluated per animal, and each point was classified according to the following parameters: healthy epithelium, prostatic intraepithelial neoplasia (PIN), atrophic epithelium, acini lumen, fibromuscular layer and inflammatory infiltrates. Thus, the percentage of each parameter for each experimental group was established based on the total number of intersections. The numbers of microacini and well-differentiated adenocarcinoma foci were quantified in 10 random fields per animal at 400× magnification. The identification of the above-described prostatic features was based on the descriptions made by Billis,³⁸ De Marzo *et al.*,³⁹ Kido *et al.*,⁴⁰ and Roy-Burman *et al.*⁴¹

Immunohistochemistry

The ventral prostates from the same animals used in the morphological analysis were sectioned into 5 µm thick slices using a micrometer (Hyrax M60, Zeiss, Germany) and placed on silanized slides for analysis. The protocol used was previously described by Montico *et al.*,¹⁰ using the following antibodies for antigen detection: rabbit polyclonal AR (sc-816 – Santa Cruz Biotechnology, Santa Cruz, CA), mouse monoclonal ERα (sc-71064 – Santa Cruz Biotechnology, Santa Cruz, CA), mouse monoclonal VEGF (sc-53462 – Santa Cruz Biotechnology, Santa Cruz, CA), rabbit polyclonal CD31 (sc-1506 – Santa Cruz Biotechnology, Santa Cruz, CA) and mouse monoclonal endostatin (ab 64569 – Abcam, Cambridge, MA). The slides were incubated for 2 hours with the following HRP-conjugated secondary antibodies: goat anti-mouse IgG (W4021, Promega Corporation, Madison, WI, USA) or goat anti-rabbit IgG (W4018, Promega Corporation, Madison, WI, USA).

Diaminobenzidine (Sigma-Aldrich) was used to detect the activity of the peroxidase conjugated with the secondary antibodies, forming a brown precipitate. Harris' hematoxylin was used for counter-staining.

After that, 10 random fields were captured (400× magnification) per animal using a Nikon Eclipse E-400 microscope (Nikon, Tokyo, Japan) with the NIS-Elements software. The immunostaining frequency was graded on a 0–3 scale, according to the percentage of positive staining areas: the percentage of positive areas for each antigen: 0 (absence of immunostaining) 0%; 1 (weak immunostaining) 1–33%; 2 (moderate immunostaining) 34–66%; and 3 (intense immunostaining) more than 66%.¹⁰ This methodology was also performed without the primary antibodies in all immunohistochemical analyses, used as negative controls.

Determination of the microvessel density (MVD)

The MVD was determined by CD31 immunostaining performed in five animals per group. Ten random images (400× magnification) were captured per animal using a Nikon Eclipse E-400 microscope (Nikon, Tokyo, Japan) with the NIS-Elements software. The mean MVD was determined by the average count of microvessels present in the 10 fields. The maximum MVD was considered to be the highest density in a field per animal. These protocols followed the methods described by Weidner *et al.*⁴² and Hochberg *et al.*⁴³

Western blotting

Five ventral prostate samples per group were frozen at –80 °C and used in this analysis. These fragments were homogenized in a RIPA (radio-immunoprecipitation assay) buffer containing a protease inhibitor cocktail (Sigma-Aldrich, St Louis, MO, USA) using a Polytron homogenizer (Kinematica). The protein concentration of each sample was determined using the Bradford reagent (Bio-Rad Laboratories, Hercules, CA, USA). An aliquot of each sample containing 50 µg of protein was applied in SDS-polyacrylamide gel under reducing conditions and transferred to nitrocellulose membranes (Amersham). This experiment followed the protocol previously described by Kido *et al.*⁴⁴ The membranes were blocked with bovine serum albumin (1%–5%), and incubated overnight with the following primary antibodies: rabbit polyclonal AR (sc-816 – Santa Cruz Biotechnology, Santa Cruz, CA), mouse monoclonal ERα (sc-71064 – Santa Cruz Biotechnology, Santa Cruz, CA), rabbit polyclonal aromatase (ab 19995 – Abcam, Cambridge, MA), mouse monoclonal VEGF (sc-53462 – Santa Cruz Biotechnology, Santa Cruz, CA), mouse monoclonal PCNA (ab 29 – Abcam, Cambridge, MA) and mouse monoclonal β-actin (sc-81178 – Santa Cruz Biotechnology, Santa Cruz, CA). Then, the membranes were washed with Tris-buffered saline and Tween 20, and incubated for 2 hours with the following HRP-conjugated secondary antibodies: goat anti-mouse IgG (W4021, Promega Corporation, Madison, WI, USA) or goat anti-rabbit IgG (W4018, Promega Corporation, Madison, WI, USA). The membranes were incubated with a chemiluminescence solution (Pierce Biotechnology Western Blotting) for

5 minutes in order to detect the bands, which were captured using a G-Box Chemi system with the GeneSnap (Syngene, Cambridge, UK) image acquisition software. The band intensity was quantified by densitometry using ImageJ software. The results were expressed as mean percentage correlated to the β -actin band intensity.

Statistical analyses

The statistical analyses of the morphological, MVD, and western blotting evaluations were carried out by analysis of variance (one-way ANOVA) followed by Tukey's multiple range post-test. A significance limit of $p < 0.05$ was considered. All these data were expressed as mean \pm standard deviation.⁴⁵ Pearson's correlation test was performed to obtain correlation values (r) between the PIN frequency and the cell proliferation value, measured by means of PCNA relative quantification.

Results

The PJE prevented lesions in the prostates of both aging and HFD-fed aging mice

PJE treatment led to the reduction of morphological damage in the prostates of aging mice. Both JAGI and JAGII groups showed a low relative percentage of epithelium atrophy (4.46% and 3.62%; $p = 0.0072$), PIN (5.22% and 4.64%; $p = 0.0024$), and inflammatory cells (0.11% and 0.04%; $p = 0.0161$) and a reduction in the number of well-differentiated adenocarcinoma foci (2.17 and 1.4; $p = 0.0077$) compared to the AG group (6.6%, 11.14%, 0.8% and 4.33, respectively) (Fig. 1B, C, F and G). The increase in the relative percentage of healthy epithelium (21.83%; $p = 0.0075$) in the JAGII group was identified by comparing this group to the JAGI (13.63%) and AG (12.61%) groups, pointing out the beneficial dose-dependent effect of the PJE on the ventral prostate (Fig. 1A). Moreover, only treatment with a high dose of the PJE (JAGII group) reduced the fibromuscular layer thickness (11.35%; $p = 0.0162$) in relation to the AG group (15.33%) (Fig. 1E). Fig. 2(J–O) show the representative images of the morphological pattern observed in the prostates of the JAG I and JAG II groups.

Both the groups treated with the HFD and the PJE (HfJAGI and HfJAGII groups) showed an increase in the relative percentage of healthy epithelium (13.31% and 19.70%; $p = 0.0002$) and acini lumen (59.36% and 63.36%; $p = 0.0049$) compared to the HfAG group (6.72% and 38.86%, respectively) (Fig. 1A and D). Moreover, the HfJAGI and HfJAGII groups demonstrated a low relative percentage of PIN (7.73% and 2.78%; $p = 0.0002$), in addition to a reduction in the number of foci of well-differentiated adenocarcinoma (4.0 and 2.6; $p = 0.0002$) and in the number of microacini (2.67 and 2.67; $p = 0.0052$) in relation to the HfAG group (22.89%, 6.67 foci and 6.33 microacini, respectively) (Fig. 1B, G and H). The dose-dependent effect of the PJE could be confirmed by the relative percentage of PIN once this parameter was reduced in the HfJAGII group compared to the HfJAGI group (7.73% and 2.78%; $p = 0.0052$) (Fig. 1B). The relative percentage of atrophic epithelium

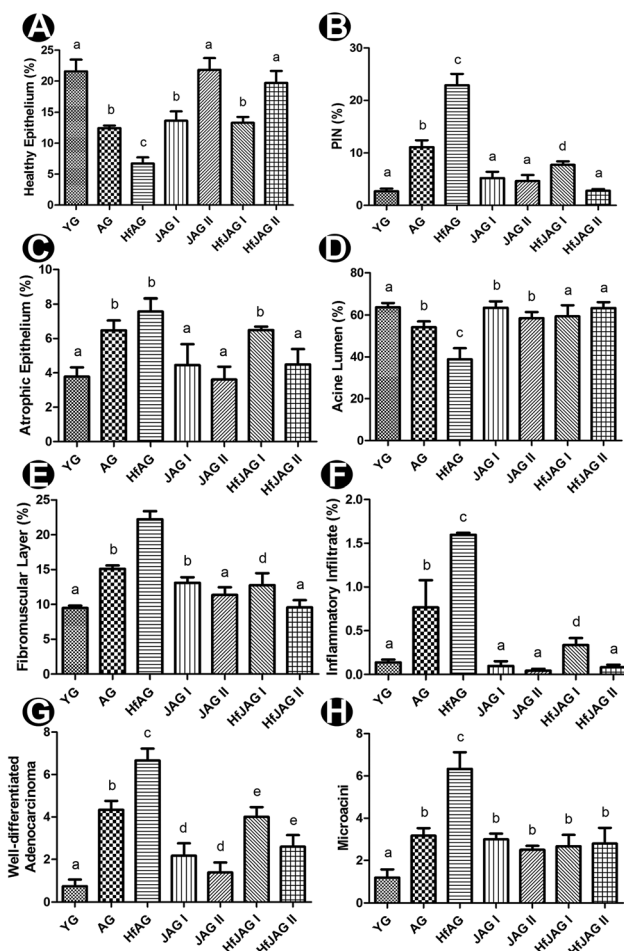


Fig. 1 Analysis of histopathological parameters in the ventral prostate of mice from different experimental groups. (A) Healthy Epithelium (%). (B) Prostatic Intraepithelial Neoplasia (%). (C) Atrophic Epithelium (%). (D) Acine Lumen (%). (E) Fibromuscular Layer (%). (F) Inflammatory Infiltrate (%). (G) Number of Well-differentiated Adenocarcinoma. (H) Number of Microacini. Different lower case letter indicates a statistical difference.

decreased only in the HfJAGII group (4.50%; $p = 0.0002$) in relation to the HfJAGI (6.5%) and HfAG (7.59%) groups, which is another indication of the dose-dependent effect of the PJE (Fig. 1C). The prostatic stroma showed a thin fibromuscular layer around the acini (12.76% and 9.58%; $p = 0.0002$) and a decrease in the relative percentage of inflammatory cells (0.34% and 0.08%; $p < 0.0001$) in both the HfJAGI and HfJAGII groups compared to the HfAG group (22.20% and 1.74%, respectively) (Fig. 1E and F). Moreover, the relative percentage of inflammatory cells was even lower in the HfJAGII group than in the HfJAGI group ($p < 0.001$) (Fig. 1F). Fig. 2(P–U) show the representative images of the morphological pattern observed in the prostates of the HfJAGI and HfJAGII groups.

The PJE decreased cell proliferation

Both PJE treatments were effective, reducing the proliferation rate in both the JAGI and JAGII groups (47.4% and 48.07%; $p = 0.0135$) compared to the AG group (110.45%), and also in both

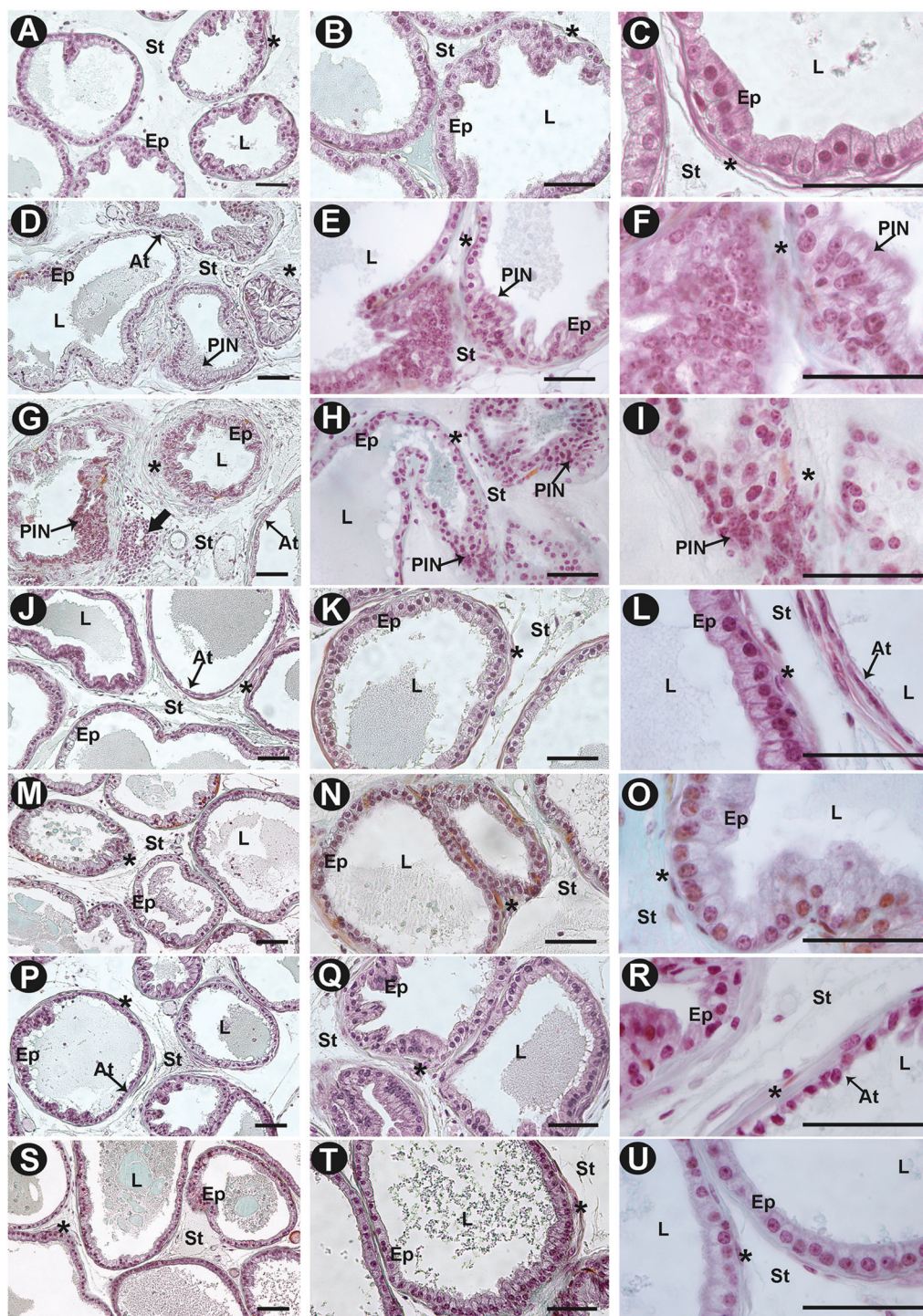


Fig. 2 Photomicrographs of the ventral prostate morphology in the experimental groups. (A–C) YG group. (D–F) AG group. (G–I) HfAG group. (J–L) JAGI group. (M–O) JAGII group. (P–R) HfJAGI group. (S–U) HfJAGII group. Scale bar = 50 μ m. (Ep): epithelium; (St): stroma; (L): lumen; (*): fibromuscular layer; (thin arrow): prostatic intraepithelial neoplasia; (thick arrow): inflammatory infiltrate. Sections stained with Masson's Trichrome (A–U). Representative photomicrographs of the ventral prostate morphology of the other animals from each experimental group can be seen in Fig. 1 of the ESI.†

the HfAGI and HfAGII groups (48.25% and 43.8%; $p = 0.0005$) compared to the HfAG group (125.47%) (Fig. 3A). In order to verify a possible correlation between the PIN frequency and PCNA levels, Pearson's coefficient was determined, which showed a high and positive correlation ($r = 0.9104$; $p = 0.0044$).

The PJE favored the steroid hormone balance, interfering in ER α signaling

The results obtained in aging mice treated with the PJE confirmed the dose-dependent effect of the extract on hormonal

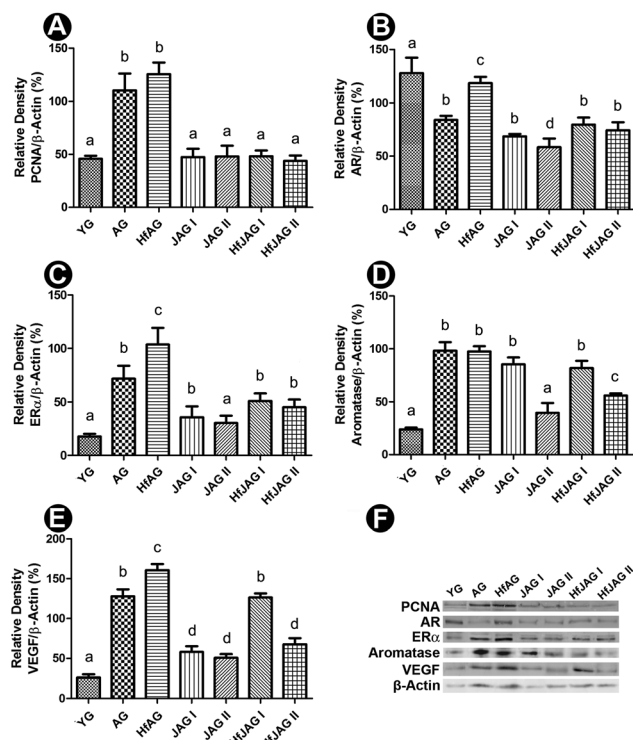


Fig. 3 Western-blotting analysis of PCNA, AR, ER α , aromatase and VEGF levels in the ventral prostates of mice from different experimental groups. (A) Relative frequency of PCNA. (B) Relative frequency of AR. (C) Relative frequency of ER α . (D) Relative frequency of aromatase. (E) Relative frequency of VEGF. (F) Illustration of the band pattern analyzed for the different molecules quantified and for the endogenous standard used. Different lowercase letters indicate a statistical difference. Illustrations of the other bands quantified for each molecule can be seen in Fig. 7 of the ESI.†

response, reinforcing its action in the signaling of steroid hormones. Both the JAG I and JAG II groups demonstrated a low immunoreactivity of ER α (weak immunostaining) in relation to the AG group. Nevertheless, only a high dose of the PJE led to a decrease in the relative density of AR (58.40%; $p = 0.0240$) and ER α (30.29%; $p = 0.0004$) in the JAG II group compared to the AG group (84.09% and 71.58%, respectively). Moreover, there was a reduction in the relative density of aromatase in the JAG II group (39.54%; $p = 0.0038$) compared to the JAG I (81.74%) and AG (98.13%) groups (Fig. 3D). Fig. 4(D, E, K and L) show the representative images of the AR and ER α immunostaining pattern observed in the prostates of the JAG I and JAG II groups.

Both doses of the PJE, in the HfJAG I and HfJAG II groups, were effective in reducing the relative density and the immunoreactivity of AR (19.65% and 74.42%; $p = 0.0023$; weak immunostaining) and ER α (50.93% and 45.12%; $p < 0.0001$; weak immunostaining) compared to the HfAG group (118.46% and 103.52%, respectively) (Fig. 3B and C; Table 1). The dose-dependent effect of the PJE was observed in the relative density of aromatase once a low relative density of this enzyme was confirmed in the HfJAG II group (55.94%; $p = 0.0020$) in

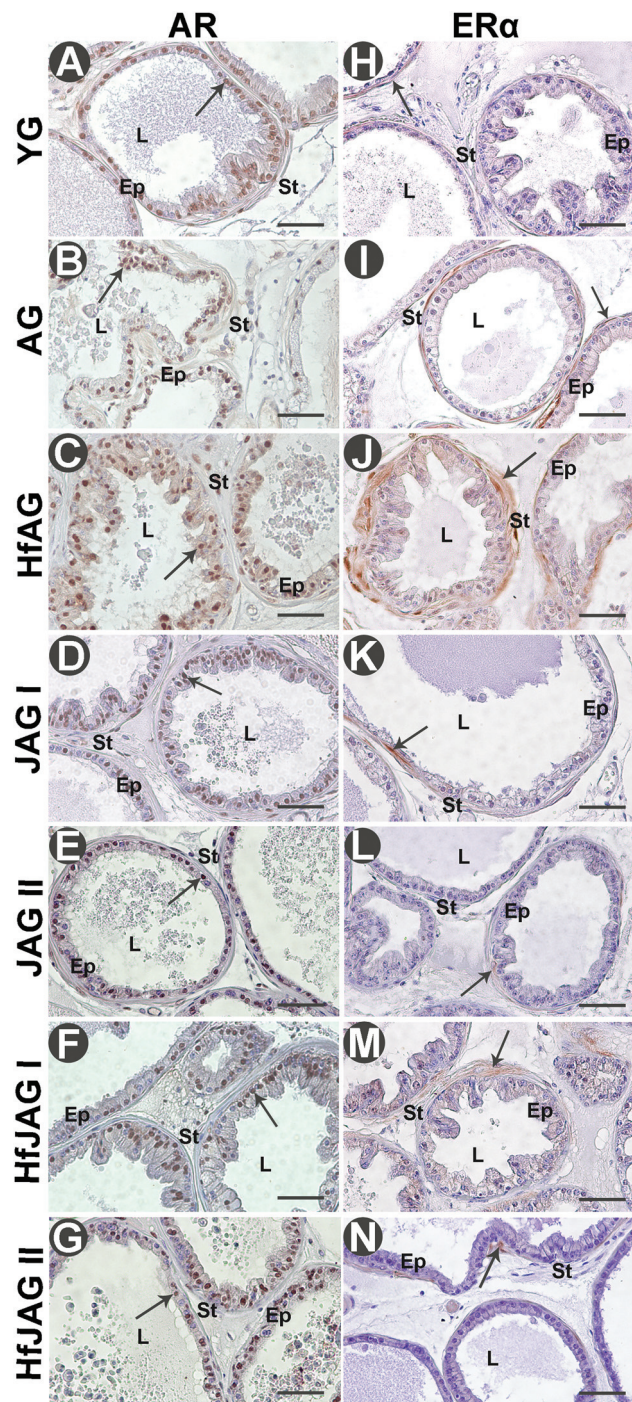


Fig. 4 Immunoreactivity of AR and ER α in the ventral prostates of mice from the YG group (A and H), AG group (B and I), HfAG group (C and J), JAG I group (D and K), JAG II group (E and L), HfJAG I group (F and M) and HfJAG II group (G and N). Scale bar = 50 μ m. (Ep): epithelium; (St): stroma; (L): lumen; (thin arrow): immunostaining. Epithelial and stromal immunoreactivity was graded as described in Table 1. Representative photomicrographs of the ventral prostate AR and ER α immunoreactivity observed in the other animals from each experimental group can be seen in Fig. 2 and 3 of the ESI.†

Table 1 Immunoreactivity positive frequency in the experimental groups

		Experimental groups						
		YG	AG	HfAG	JAGI	JAGII	HfJAGI	HfJAGII
AR	Ep	3	2	3	2	2	2	2
	St	3	2	3	2	2	2	2
ER α	Ep	0	0	0	0	0	0	0
	St	1	2	3	1	1	2	2
VEGF	Ep	1	3	3	3	2	1	1
	St	1	2	3	2	2	1	1
Endostatin	Ep	3	2	1	3	3	3	3
	St	3	1	1	1	3	2	3

Distribution according to predominant range: 0 (0% – absence of immunostaining), 1 ($\leq 33\%$ – weak immunostaining), 2 (33–66% – moderate immunostaining), and 3 ($\geq 66\%$ – intense immunostaining). Ep: epithelium; St: stroma.

relation to the HfJAGI (81.74%) and HfAG (97.41%) groups (Fig. 3D). Fig. 4(F, G, M and N) show the representative images of the AR and ER α immunostaining pattern observed in the prostates of the HfJAGI and HfJAGII groups.

PJE treatment downregulated the angiogenesis process response

The treatment with the PJE downregulated the angiogenic pathways, in a dose-dependent manner, in the different aging experimental groups. The JAGI and JAGII groups showed a reduction in the relative density of VEGF (58.09% and 50.81%; $p < 0.0001$) and mean MVD (7.7 and 6.7; $p = 0.0013$), besides increased epithelium immunolabeling of endostatin (intense immunostaining) compared to the AG group (128% and 12.9, respectively) (Fig. 3E; Tables 1 and 2). The dose-dependent effect of the PJE was confirmed since only a high dose of the PJE, in the JAGII group, reduced the epithelium immunolabeling of VEGF (moderate immunostaining) and also increased the stromal immunoreactivity of endostatin (intense immunostaining) in relation to the AG group (Table 1). Fig. 5(D, E, K, L, R and S) show the representative images of the CD31, VEGF and endostatin immunostaining pattern observed in the prostates of the JAGI and JAGII groups.

Both doses of the PJE, in the HfJAGI and HfJAGII groups, reduced the relative density and the immunolabeling of VEGF (126.48% and 67.68%; $p < 0.0001$; weak immunostaining) in relation to the HfAG group (160.79%) (Fig. 3E; Table 1). In addition, the HfJAGI and HfJAGII groups also demonstrated a decrease in the mean and maximum MVD (8.7 and 5.3 mean MVD; $p = 0.0092$; 15.6 and 11.0 maximum MVD; $p = 0.0032$) and an increase in the immunolabeling of endostatin in both

the epithelium and stroma (intense immunostaining) in relation to the HfAG group (13.3 mean MVD; 19.7 maximum MVD) (Tables 1 and 2). The dose-dependent effect of the PJE was reinforced by the reduction in the maximum MVD ($p = 0.0032$) and in the relative density of VEGF ($p < 0.0001$) in addition to the improved stromal immunoreactivity of endostatin (intense immunostaining) in the HfJAGII group compared to the HfJAGI group (Fig. 3E; Tables 1 and 2). Fig. 5(F, G, M, N, T and U) show the representative images of the CD31, VEGF and endostatin immunostaining pattern observed in the prostates of the HfJAGI and HfJAGII groups.

The HFD intensified hormonal imbalance and angiogenesis in the prostate during late life, increasing the lesion incidence in this gland

The morphological analysis of the AG group showed a reduction in the relative percentage of healthy epithelium (12.61%; $p = 0.0001$) and acinar lumen (53.52%; $p = 0.0092$) compared to the YG group (21.57% and 62.33%, respectively) (Fig. 1A and D). Moreover, the AG group showed an increase in the relative percentage of epithelium atrophy (6.60%; $p = 0.0004$) and PIN (11.14%; $p = 0.0003$) and more well-differentiated adenocarcinoma foci (4.33; $p = 0.0114$), a large number of microacini (3.17; $p = 0.024$) and a proliferative rate improvement (110.45%; $p = 0.0153$) in relation to the YG group (3.78%, 2.68%, 0.75 foci, 1.2 microacini and 45.84%, respectively) (Fig. 1B, C, G, H and 3A). A hypertrophic and hyperplastic prostatic stroma was observed in the AG group. The presence of a thick fibromuscular layer around the acini (15.33%; $p = 0.0103$) and a high relative percentage of inflammatory cells (0.80%; $p = 0.04$) were confirmed in this group compared to

Table 2 Determination of the microvessel density (MVD) (mean \pm SD)

	Experimental Groups						
	YG	AG	HfAG	JAGI	JAGII	HfJAGI	HfJAGII
Mean MVD	6.8 \pm 1.2 ^a	12.9 \pm 1.7 ^b	13.3 \pm 3.1 ^b	7.7 \pm 1.7 ^a	6.7 \pm 2.3 ^a	8.7 \pm 2.1 ^c	5.3 \pm 0.1 ^a
Maximum MVD	11.0 \pm 2.5 ^a	19.6 \pm 1.5 ^b	19.7 \pm 1.5 ^b	12.2 \pm 2.8 ^a	11.7 \pm 4.1 ^a	15.6 \pm 1.9 ^c	11.0 \pm 1.4 ^a

Different lowercase letters indicate a statistical difference.

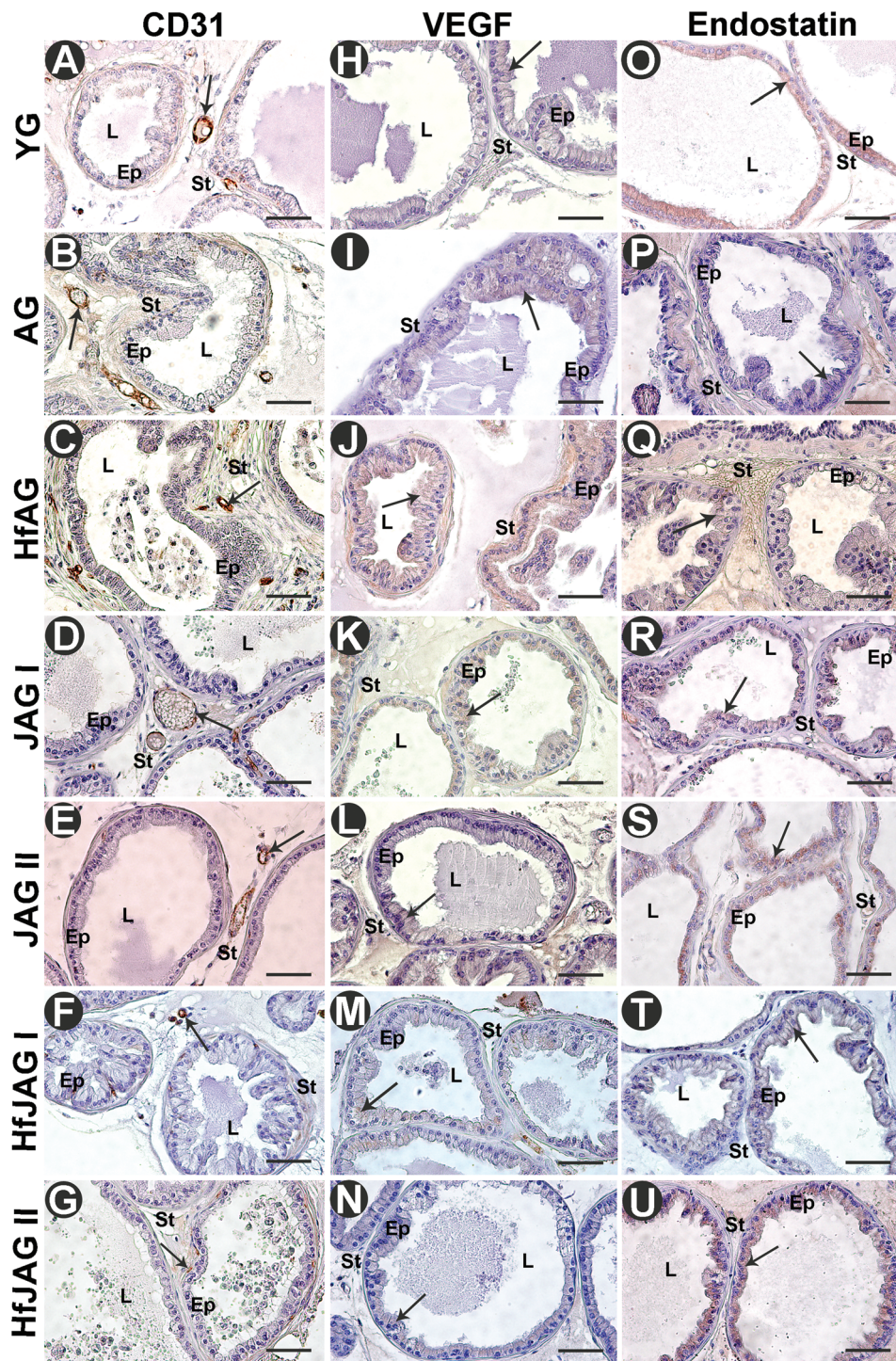


Fig. 5 Immunoreactivity of CD31, VEGF, and endostatin in the ventral prostates of mice from the YG group (A, H and O), AG group (B, I and P), HfAG group (C, J and Q), JAG I group (D, K and R), JAG II group (E, L and S), HfJAG I group (F, M and T) and HfJAG II group (G, N and U). Scale bar = 50 μ m. (Ep): epithelium; (St): stroma; (L): lumen; (thin arrow): immunostaining. Epithelial and stromal immunoreactivity gradation and microvessel determination are given in Tables 1 and 2, respectively. Representative photomicrographs of the ventral prostate VEGF, endostatin and CD31 immunoreactivity observed in the other animals from each experimental group can be seen in Fig. 4, 5 and 6 of the ESI.†

the YG group (9.5% and 0.14%, respectively). Fig. 2(A–F) show the representative images of the morphological pattern observed in the prostates of the YG and AG groups.

HFD-fed aging mice (the HfAG group) showed intensified morphological alterations, such as an increase in the relative percentage of PIN (22.89%; $p = 0.0026$), in the number of well-

differentiated adenocarcinoma foci (6.67; $p = 0.0075$) and in the number of microacini (6.33; $p = 0.0015$) in relation to the AG group (11.14%, 4.33 foci and 3.17 microacini, respectively) (Fig. 1B, G and H). In addition, the relative percentage of epithelium atrophy (7.59%; $p = 0.9183$) and the proliferative rate (125.41%; $p = 4761$) in the HfAG group were as high as those in the AG group (6.6% and 110.45%) (Fig. 1C and 3A). These alterations were associated with a reduction in the relative percentage of healthy epithelium (6.72%; $p = 0.0037$) and acinar lumen (38.86%; $p = 0.0154$) in the HfAG group compared to the AG group (12.61% and 53.52%, respectively) (Fig. 1A and D). Also, the HfAG group showed a hypertrophic and hyperplastic prostatic stroma, where a thick fibromuscular layer around the acini (22.20%; $p = 0.0077$) and a high relative percentage of inflammatory cells (1.74%; $p = 0.0227$) were observed compared to the AG group (15.33% and 0.8%, respectively) (Fig. 1E and F). Fig. 2(G–I) show the representative images of the morphological pattern observed in the prostates of the HfAG group.

The aging mice, in the AG group, showed alterations in the hormone-related molecules, such as a reduction in the relative density of AR and its immunoexpression (84.09%; $p = 0.0266$; moderate immunostaining) compared to the YG group (127.84%) (Fig. 3B; Table 1). Moreover, the AG group demonstrated a high relative density of aromatase (98.13%; $p = 0.0001$) in addition to an increase in the relative density and immunoexpression of ER α (71.58%; $p = 0.0047$; moderate immunostaining) compared to the YG group (23.78% and 17.73%, respectively) (Fig. 3C and D; Table 1). Fig. 4(A, B, H and I) show the representative images of the AR and ER α immunostaining pattern observed in the prostates of the YG and AG groups.

The HFD intake by aging mice increased the relative density of AR (118.46%; $p = 0.0028$) and ER α (103.52%; $p = 0.0332$) in the prostates of mice from the HfAG group compared to the AG group (84.89% and 71.58%, respectively) (Fig. 3B and C). These data are in agreement with those obtained in the immunohistochemistry evaluation, which showed increased epithelial and stromal immunoreactivity of AR (intense immunostaining) and ER α (intense immunostaining) in the HfAG group compared to the AG group (Table 1). The relative density of aromatase in the HfAG group (97.41%; $p = 9397$) was as high as that in the AG group (98.13%) (Fig. 3D). Fig. 4(C and J) show the representative images of the AR and ER α immunostaining pattern observed in the prostates of the HfAG group.

Regarding the angiogenesis process, the AG group demonstrated a high relative density and immunoexpression of VEGF (128%; $p < 0.0001$; intense epithelium immunostaining and moderate stromal immunostaining) in addition to an increase in the mean MVD (12.9; $p < 0.0001$) compared to the YG group (26.14%; 6.8 mean MVD, respectively) (Fig. 3E; Tables 1 and 2). Also, a decrease in the immunoexpression of endostatin was observed in the AG group (moderate epithelium immunostaining and weak stromal immunostaining) in relation to the YG group (Table 1). Fig. 5(A, B, H, I, O and P) show the representative images of the CD31, VEGF and endostatin immunostaining pattern observed in the prostates of the AG and YG groups.

The HFD intake by aging mice increased the relative density of VEGF in the HfAG group (160.79%; $p = 0.0284$) compared to the AG group (128%) (Fig. 3E). These data are in agreement with those obtained in the immunohistochemistry evaluation, which showed high stromal immunolabeling of VEGF in the HfAG group (intense immunostaining) compared to the AG group (Fig. 5J; Table 1). Moreover, the HfAG group showed a low epithelium immunolabeling of endostatin (weak immunostaining) in relation to the AG group (Table 1). Fig. 5 (C, J and Q) show the representative images of the CD31, VEGF and endostatin immunostaining pattern observed in the prostates of the HfAG group.

Discussion

The study herein presented, for the first time, the positive effect of the jaboticaba extract (PJE) on the prostatic disturbance induced by aging *in vivo*. The results showed that the PJE promoted a dose-dependent hormonal and angiogenic homeostasis in the ventral prostates of aging mice associated with or not associated with HFD intake. These effects were related to the prevention of prostatic microenvironment imbalance and cell proliferation reduction, leading to the maintenance of the healthy morphology of this gland in aging or HFD-fed aging mice.

A previous study by our research group focused on the development of the PJE and characterization of its bioactive compounds, indicating that the PJE has a similar phenolic profile to that found in the literature.^{21,35,46} In addition, the PJE has a high phenolic and flavonoid content, and also a high *in vitro* antioxidant capacity compared to methanolic or aqueous jaboticaba extracts^{47,48} and other fruit extracts such as grape peel, mulberry and raspberry extracts.^{49–51} The patented method used in its preparation and the solvent type and concentration are some important aspects which contributed to the maintenance of the high phenolic content in the PJE and its improved *in vitro* antioxidant capacity.²¹ Thus, we believe that the large amount and variety of bioactive compounds present in the PJE contributed to the broad, synergic and positive effects of the PJE observed in the present study.

The PJE positive dose-dependent action was seen herein by the intense effective response of the damaged prostate tissue to the treatment with a high dose of the PJE in both aging and HFD-fed aging mice. Also, our results showed that the PJE capacity to reduce prostatic lesions is associated with its effect in reducing cell proliferation in this gland. One of the polyphenol pathways that could have an involvement in these findings is through cell cycle arrest and apoptosis stimulation, which occurred preferentially *via* the p53-dependent pathway, regulating both p21 and Bax molecules.²³ In addition, polyphenols have the capacity to reduce the expression of the MAPK signaling pathway molecules that trigger the transcription of genes related to cell proliferation.²⁸ Thus, polyphenols can regulate the expression of molecules that induce cell proliferation, such as steroid hormones and mitogenic factors, at the ligand and

receptor level, preventing the development of prostatic proliferative lesions.²⁸

This is the first report demonstrating that treatment with the PJE interferes in prostatic steroid hormone pathways altered by aging, reducing the levels of AR, ER α and aromatase. Based on the literature,^{23,28} we believe that these effects could have a direct implication in the reduction of cell proliferation rates, contributing to the reduction of epithelial changes, malignant lesions and stromal hypertrophy, triggering the normal epithelial–stromal interaction and the morphological maintenance in aging or HFD-fed aging mice.

Nevertheless, besides the lack of data regarding polyphenol action on the prostates of aging mice, there are some studies showing that polyphenols from different sources can reduce AR expression in cell culture or in rodent prostate cancer models.^{28,29,52} According to different authors, the main mechanisms by which polyphenols reduce the level of AR could be summarized as follows: (i) reduction of testosterone production in Leydig cells; (ii) suppression of AR expression by affecting upstream pathways related to inflammation or oxidative stress; (iii) interference in AR nuclear translocation; and (iv) reduction of weight gain and, consequently, decreasing leptin secretion, which regulates the circulation of the sex steroids.^{53–58} Corroborating these data, a previous study by our group confirmed that the PJE, the same used herein, had the ability to reduce the weight gain of aging mice, leading to anti-inflammatory and antioxidant properties.²¹ Thus, we could suggest that the broader capacity of the PJE to interfere in interconnected pathways related to the accumulation of body fat, inflammation, and oxidation could have a significant role in the reduction of AR in aging or HFD-fed aging mouse prostates observed herein, possibly regulating the androgen action at the receptor level.

Furthermore, polyphenols have been described as enzyme inhibitors, since they can interact with the binding site of enzymes, reducing their activity.⁵⁹ The literature shows that both aging and obesity are related to the stimulation of aromatase, altering the prostatic hormonal balance and creating a supportive microenvironment, which can favor malignant prostate growth.^{6,8} Thus, the capacity of the PJE to reduce the aromatase level herein seems to be an important strategy to control the hormonal imbalance in this gland. Previous studies on the adipose tissue of HFD-fed mice and on breast cancer cells showed that polyphenols reduced the level of aromatase and suggested that it was related to a decrease in the level of estrogen and cell proliferation.^{8,60} According to Wang *et al.*,⁶¹ polyphenols such as resveratrol can reduce the expression of aromatase by interfering with a promoter of its transcription in breast cancer cell culture. Therefore, the ability of polyphenol to interfere in the expression or activity of aromatase could have contributed to reduce its levels in the aging or HFD-fed aging mouse prostates after PJE treatment. The low level of AR observed herein could suggest a low level of androgen circulation, which may also collaborate towards the reduction of this enzyme.

The increased aromatization in different tissues has been linked to a high estrogen level in different organs.^{8,62} High

levels of ER α , which were directly associated with cell proliferation, mechanisms of cell migration, and cancer onset, were confirmed in the prostates of aging and obese rodents.^{40,63} Interestingly, the reduction of aromatase by resveratrol in breast cancer cell culture was also associated with the downregulation of phospho-ERK-1/2 estrogen activated signaling, suggesting low levels of this hormone.⁶¹ However, a previous study, evaluating a prostate cancer transgenic mouse model, described that the polyphenol epigallocatechin-3-gallate did not play a significant role in the ER α action mechanism.²⁸ In the present study, we believe that a broad spectrum of polyphenols in the PJE exerted a synergic action towards prostate hormone homeostasis. The low levels of aromatase decreased the androgen conversion into estrogen, probably reducing the level of this hormone, favoring ER α reduction. Thus, our results demonstrated the capacity of the PJE to interfere in the estrogen pathway by means of low levels of ER α . This effect seems to be a differential of the PJE action, reinforcing its therapeutic effect to prevent the development of malignant lesions in the prostate.

Our present results also revealed that both doses of the PJE presented an antiangiogenic effect, which is crucial to prevent cell migration and invasion pathways in the prostates of aging or HFD-fed aging mice.^{19,64} Several angiogenesis inhibitors and polyphenols, from different sources, have demonstrated the ability to prevent angiogenesis in cell cultures and in *in vivo* prostate cancer models, mainly by decreasing VEGF and MVD.^{10,30,65} One important mechanism for angiogenesis downregulation by polyphenols is their capacity to inhibit VEGF binding to its receptor.^{66,67} Nevertheless, these results were accompanied by endostatin immunoexpression reduction.¹⁰ Endostatin can interact with other molecules involved in the VEGF signaling pathway, decreasing angiogenesis and cell proliferation, besides increasing the apoptotic rate.^{64,68,69} Therefore, our results suggested that the reduction of VEGF might be one of the action mechanisms of the PJE. These data possibly resulted in low MVD and angiogenesis, which were associated with low premalignant and invasive malignant lesions in the prostate. Nevertheless, the key point of our findings is that the PJE prevented the angiogenic process not only by decreasing the levels of VEGF and MVD, but also by stimulating the immunoexpression of endostatin in aging and HFD-fed aging mice. This result reinforces the broader action of the PJE and its advantageous effect on the angiogenesis process. We encourage the development of future research focusing on the mechanisms of the PJE to improve the expression of endostatin in order to clarify this perspective.

In addition, a disturbance in androgen homeostasis can interfere with the vascular stability and the angiogenic process.^{10,70} The endothelial cells also express AR, regulating the cellular mechanism of integrity, viability and proliferation.^{10,70} A previous study demonstrated that the treatment with finasteride reduced the levels of VEGF and MVD in aging mice by inhibiting the activity of 5 α -reductase.¹⁰ Thus, considering the effects of the PJE on hormonal receptors, we could suggest a possible influence of the PJE on the vascular

endothelium, decreasing the angiogenic process, which could be related to the reestablishment of the hormonal balance in both aging and HFD-fed aging mice.

There are several studies in the literature demonstrating the deleterious effects of a HFD on the prostate.^{19,20,22} Nevertheless, this is the first research that shows the effect of HFD intake on the prostates of aging mice, which was characterized by typical harmful changes during late life. The intensification of prostatic damage in HFD-fed aging mice occurred possibly due to the association of two factors related to prostate injury. Thus, the HFD intake during aging led to a hormonal imbalance, characterizing the prostatic microenvironment favorable to the development of proliferative and invasive lesions. Also, angiogenesis increased in HFD-fed aging mice, in order to support the proliferative prostatic microenvironment triggered by HFD intake during late life. Montico *et al.*¹⁰ showed that the angiogenesis process during aging is compatible with the neovascularization observed in prostate cancer in a transgenic mouse model, highlighting the importance of this process in prostatic lesions in late life. Therefore, we emphasize the relevance of studies involving aging animals which will be useful to understand or mitigate the relationship between aging, increased adiposity, and prostatic lesions.

Conclusion

The broader action of the PJE involved the reestablishment of hormonal homeostasis and the reduction of the angiogenic process, which certainly contributed to the decrease of the proliferative process in this gland. Also, treatments with the PJE indicated different positive glandular responses, characterizing a tissue protection role even after the administration of a low dose of the PJE. The beneficial effect of the PJE was dose-dependent in both experimental models, considering that only a high dose of the PJE restored the healthy morphology of this gland. Therefore, the PJE can be indicated as a potential therapeutic adjuvant in the treatment or prevention of prostate malignant and pre-malignant lesions associated with aging and overweight.

Funding source

This study was funded by the National Council for Scientific and Technological Development (CNPq – 141766/2015-8) and the São Paulo Research Foundation (FAPESP – 2015/25714-1). MRMJ acknowledges CNPq (301108/2016-1 and 403328/2016-0) and FAPESP (2015/50333-1 and 2010/05262-5) for the financial support.

Ethical approval

All applicable international, national, and/or institutional guidelines for the care and use of animals were followed. All procedures performed in the studies involving animals were in

accordance with the ethical standards of the institution or practice at which the studies were conducted.

Conflicts of interest

The authors declare that they have no conflicts of interest.

Acknowledgements

The authors acknowledge the website “Mind the Graph” for the images used in the graphical abstract.

References

- 1 J. Li, *et al.*, Recent trends in prostate cancer incidence by age, cancer stage, and grade, the United States, 2001-2007, *Prostate Cancer*, 2012, **2012**, 691380–691380.
- 2 F. Bray, *et al.*, Global cancer statistics 2018: GLOBOCAN estimates of incidence and mortality worldwide for 36 cancers in 185 countries, *CA Cancer J. Clin.*, 2018, **68**, 394–424.
- 3 L. A. Kido, *et al.*, Goniiothalamine and Celecoxib Effects During Aging: Targeting Pro-Inflammatory Mediators in Chemoprevention of Prostatic Disorders, *Prostate*, 2017, **77**, 838–848.
- 4 A. Morales, Androgen replacement therapy and prostate safety, *Eur. Urol.*, 2002, **41**, 113–120.
- 5 S. M. Harman, *et al.*, Longitudinal effects of aging on serum total and free testosterone levels in healthy men. Baltimore Longitudinal Study of Aging, *J. Clin. Endocrinol. Metab.*, 2001, **86**, 724–731.
- 6 S. J. Ellem, *et al.*, Increased endogenous estrogen synthesis leads to the sequential induction of prostatic inflammation (prostatitis) and prostatic pre-malignancy, *Am. J. Pathol.*, 2009, **175**, 1187–1199.
- 7 L. O'Donnell, *et al.*, Estrogen and spermatogenesis, *Endocr. Rev.*, 2001, **22**, 289–318.
- 8 L. Polari, *et al.*, Weight gain and inflammation regulate aromatase expression in male adipose tissue, as evidenced by reporter gene activity, *Mol. Cell. Endocrinol.*, 2015, **412**, 123–130.
- 9 R. F. Silva, *et al.*, Nintedanib antiangiogenic inhibitor effectiveness in delaying adenocarcinoma progression in Transgenic Adenocarcinoma of the Mouse Prostate (TRAMP), *J. Biomed. Sci.*, 2017, **24**, 31.
- 10 F. Montico, *et al.*, Prostatic angiogenic responses in late life: antiangiogenic therapy influences and relation with the glandular microenvironment in the transgenic adenocarcinoma of mouse prostate (TRAMP) model, *Prostate*, 2015, **75**, 484–499.
- 11 R. Bianco, *et al.*, Vascular endothelial growth factor receptor-1 contributes to resistance to anti-epidermal growth factor receptor drugs in human cancer cells, *Clin. Cancer Res.*, 2008, **14**, 5069–5080.

- 12 W. J. Huss, *et al.*, Angiogenesis and prostate cancer: identification of a molecular progression switch, *Cancer Res.*, 2001, **61**, 2736–2743.
- 13 M. Papetti and I. M. Herman, Mechanisms of normal and tumor-derived angiogenesis, *Am. J. Physiol.: Cell Physiol.*, 2002, **282**, C947–C970.
- 14 N. B. Delongchamps, *et al.*, Role of vascular endothelial growth factor in prostate cancer, *Urology*, 2006, **68**, 244–248.
- 15 F. Montico, *et al.*, Angiogenic and tissue remodeling factors in the prostate of elderly rats submitted to hormonal replacement, *Anat. Rec.*, 2013, **296**, 1758–1767.
- 16 A. Schmidt, *et al.*, Differential endostatin binding to bladder, prostate and kidney tumour vessels, *BJU Int.*, 2005, **95**, 174–179.
- 17 WHO, Global Health and Aging, *World Health Organization*, 2011, 1–32.
- 18 A. Perez-Cornago, *et al.*, Tall height and obesity are associated with an increased risk of aggressive prostate cancer: results from the EPIC cohort study, *BMC Med.*, 2017, **15**, 115.
- 19 S. A. Silva, *et al.*, Prostate hyperplasia caused by long-term obesity is characterized by high deposition of extracellular matrix and increased content of MMP-9 and VEGF, *Int. J. Exp. Pathol.*, 2015, **96**, 21–30.
- 20 H. J. Yang, *et al.*, Which obesity index best correlates with prostate volume, prostate-specific antigen, and lower urinary tract symptoms?, *Urology*, 2012, **80**, 187–190.
- 21 C. A. Lamas, *et al.*, Jaboticaba extract prevents prediabetes and liver steatosis in high-fat-fed aging mice, *J. Funct. Foods*, 2018, **47**, 434–446.
- 22 C. Pelser, *et al.*, Dietary fat, fatty acids, and risk of prostate cancer in the NIH-AARP diet and health study, *Cancer Epidemiol., Biomarkers Prev.*, 2013, **22**, 697–707.
- 23 T. Castelli, *et al.*, Metabolic syndrome and prostatic disease: potentially role of polyphenols in preventive strategies. A review, *Int. Braz. J. Urol.*, 2016, **42**, 422–430.
- 24 Y. W. Park, *et al.*, The relationship between lower urinary tract symptoms/benign prostatic hyperplasia and the number of components of metabolic syndrome, *Urology*, 2013, **82**, 674–679.
- 25 A. Nicolai, *et al.*, Heme oxygenase-1 induction remodels adipose tissue and improves insulin sensitivity in obesity-induced diabetic rats, *Hypertension*, 2009, **53**, 508–515.
- 26 L. Vanella, *et al.*, Correlation between lipid profile and heme oxygenase system in patients with benign prostatic hyperplasia, *Urology*, 2014, **83**, 1444.
- 27 A. Bruni-Cardoso, *et al.*, Localized matrix metalloproteinase (MMP)-2 and MMP-9 activity in the rat ventral prostate during the first week of postnatal development, *Histochem. Cell Biol.*, 2008, **129**, 805–815.
- 28 C. E. Harper, *et al.*, Epigallocatechin-3-Gallate suppresses early stage, but not late stage prostate cancer in TRAMP mice: mechanisms of action, *Prostate*, 2007, **67**, 1576–1589.
- 29 G. Sharmila, *et al.*, Chemopreventive effect of quercetin, a natural dietary flavonoid on prostate cancer in in vivo model, *Clin. Nutr.*, 2014, **33**, 718–726.
- 30 P. Wang, *et al.*, Green tea and quercetin sensitize PC-3 xenograft prostate tumors to docetaxel chemotherapy, *J. Exp. Clin. Cancer Res.*, 2016, **35**, 73.
- 31 A. G. Batista, *et al.*, Jaboticaba berry peel intake prevents insulin-resistance-induced tau phosphorylation in mice, *Mol. Nutr. Food Res.*, 2017, **61**, 1600952.
- 32 C. A. Lamas, *et al.*, Grape juice concentrate alleviates epididymis and sperm damage in cadmium-intoxicated rats, *Int. J. Exp. Pathol.*, 2017, **98**, 86–99.
- 33 J. C. Chamcheu, *et al.*, Graviola (*Annona muricata*) Exerts Anti-Proliferative, Anti-Clonogenic and Pro-Apoptotic Effects in Human Non-Melanoma Skin Cancer UW-BCC1 and A431 Cells In Vitro: Involvement of Hedgehog Signaling, *Int. J. Mol. Sci.*, 2018, **19**, 1791.
- 34 S. A. Lenquiste, *et al.*, Freeze-dried jaboticaba peel added to high-fat diet increases HDL-cholesterol and improves insulin resistance in obese rats, *Food Res. Int.*, 2012, **49**, 153–160.
- 35 M. Plaza, *et al.*, Characterization of antioxidant polyphenols from *Myrciaria jaboticaba* peel and their effects on glucose metabolism and antioxidant status: A pilot clinical study, *Food Chem.*, 2016, **211**, 185–197.
- 36 M. R. Maróstica Junior, *et al.*, *Composition comprising jaboticaba extract, and its use*, *Brasil Pat*, BR 1020170054624, 2017.
- 37 A. M. Basseggio, *et al.*, Jaboticaba peel extract decrease autophagy in white adipose tissue and prevents metabolic disorders in mice fed with a high-fat diet, *PharmaNutrition*, 2018, **6**, 147–156.
- 38 A. Billis, *Prostate surgical pathology*, Campinas, IDB, 1st edn, 2003, p. 252. ISBN: 85-89233-06-5.
- 39 A. M. De Marzo, *et al.*, Proliferative inflammatory atrophy of the prostate: implications for prostatic carcinogenesis, *Am. J. Pathol.*, 1999, **155**, 1985–1992.
- 40 L. A. Kido, *et al.*, Antiangiogenic and finasteride therapies: responses of the prostate microenvironment in elderly mice, *Life Sci.*, 2014, **106**, 58–70.
- 41 P. Roy-Burman, *et al.*, Genetically defined mouse models that mimic natural aspects of human prostate cancer development, *Endocr.-Relat. Cancer*, 2004, **11**, 225–254.
- 42 N. Weidner, *et al.*, Tumor angiogenesis correlates with metastasis in invasive prostate carcinoma, *Am. J. Pathol.*, 1993, **143**, 401–409.
- 43 D. A. Hochberg, *et al.*, Decreased suburethral prostatic microvessel density in finasteride treated prostates: a possible mechanism for reduced bleeding in benign prostatic hyperplasia, *J. Urol.*, 2002, **167**, 1731–1733.
- 44 L. A. Kido, *et al.*, Anti-inflammatory therapies in TRAMP mice: delay in PCa progression, *Endocr.-Relat. Cancer*, 2016, **23**, 235–250.
- 45 J. Zar, *Biostatistical Analysis*, Prentice Hall, New Jersey, 1999.
- 46 K. O. P. Inada, *et al.*, Screening of the chemical composition and occurring antioxidants in jaboticaba (*Myrciaria jaboticaba*) and jussara (*Euterpe edulis*) fruits and their fractions, *J. Funct. Foods*, 2015, **17**, 422–433.
- 47 S. A. Lenquiste, *et al.*, Jaboticaba peel and jaboticaba peel aqueous extract shows in vitro and in vivo antioxidant properties in obesity model, *Food Res. Int.*, 2015, **77**, 162–170.

- 48 Â. G. Batista, *et al.*, Intake of jaboticaba peel attenuates oxidative stress in tissues and reduces circulating saturated lipids of rats with high-fat diet-induced obesity, *J. Funct. Foods*, 2014, **6**, 450–461.
- 49 I. Ky and P. L. Teissedre, Characterisation of Mediterranean grape pomace seed and skin extracts: polyphenolic content and antioxidant activity, *Molecules*, 2015, **20**, 2190–2207.
- 50 Y. Wang, *et al.*, Antidiabetic and antioxidant effects and phytochemicals of mulberry fruit (*Morus alba* L.) polyphenol enhanced extract, *PLoS One*, 2013, **8**, e71144.
- 51 A. Mezni, *et al.*, Lithium induced oxidative damage and inflammation in the rat's heart: Protective effect of grape seed and skin extract, *Biomed. Pharmacother.*, 2017, **95**, 1103–1111.
- 52 A. M. Fajardo, *et al.*, The curcumin analog ca27 down-regulates androgen receptor through an oxidative stress mediated mechanism in human prostate cancer cells, *Prostate*, 2012, **72**, 612–625.
- 53 M. F. McCarty, *et al.*, Beyond androgen deprivation: ancillary integrative strategies for targeting the androgen receptor addiction of prostate cancer, *Integr. Cancer Ther.*, 2014, **13**, 386–395.
- 54 S. Moschos, *et al.*, Leptin and reproduction: a review, *Fertil. Steril.*, 2002, **77**, 433–444.
- 55 J. L. Chan and C. S. Mantzoros, Role of leptin in energy-deprivation states: normal human physiology and clinical implications for hypothalamic amenorrhoea and anorexia nervosa, *Lancet*, 2005, **366**, 74–85.
- 56 H. S. Moon, *et al.*, Leptin's role in lipodystrophic and nonlipodystrophic insulin-resistant and diabetic individuals, *Endocr. Rev.*, 2013, **34**, 377–412.
- 57 K. Michalakis, *et al.*, Obesity in the ageing man, *Metabolism*, 2013, **62**, 1341–1349.
- 58 M. S. Figueiroa, *et al.*, Green tea polyphenols inhibit testosterone production in rat Leydig cells, *Asian J. Androl.*, 2009, **11**, 362–370.
- 59 C. G. Fraga, *et al.*, Basic biochemical mechanisms behind the health benefits of polyphenols, *Mol. Aspects Med.*, 2010, **31**, 435–445.
- 60 T. D. Way, *et al.*, Black tea polyphenol theaflavins inhibit aromatase activity and attenuate tamoxifen resistance in HER2/neu-transfected human breast cancer cells through tyrosine kinase suppression, *Eur. J. Cancer*, 2004, **40**, 2165–2174.
- 61 Y. Wang, *et al.*, A positive feedback pathway of estrogen biosynthesis in breast cancer cells is contained by resveratrol, *Toxicology*, 2008, **248**, 130–135.
- 62 S. J. Ellem and G. P. Risbridger, Aromatase and regulating the estrogen:androgen ratio in the prostate gland, *J. Steroid Biochem. Mol. Biol.*, 2010, **118**, 246–251.
- 63 D. L. Ribeiro, *et al.*, High-fat diet obesity associated with insulin resistance increases cell proliferation, estrogen receptor, and PI3 K proteins in rat ventral prostate, *J. Androl.*, 2012, **33**, 854–865.
- 64 B. K. Sim, *et al.*, Angiostatin and endostatin: endogenous inhibitors of tumor growth, *Cancer Metastasis Rev.*, 2000, **19**, 181–190.
- 65 S. Ganapathy, *et al.*, Resveratrol enhances antitumor activity of TRAIL in prostate cancer xenografts through activation of FOXO transcription factor, *PLoS One*, 2010, **5**, e15627.
- 66 M. Sousa, *et al.*, Red Raspberry Phenols Inhibit Angiogenesis: A Morphological and Subcellular Analysis Upon Human Endothelial Cells, *J. Cell. Biochem.*, 2016, **117**, 1604–1612.
- 67 C. Q. Zheng, *et al.*, Mechanisms of apple polyphenols-induced proliferation inhibiting and apoptosis in a metastatic oral adenoid cystic carcinoma cell line, *Kaohsiung J. Med. Sci.*, 2013, **29**, 239–245.
- 68 A. Abdollahi, *et al.*, Combined therapy with direct and indirect angiogenesis inhibition results in enhanced anti-angiogenic and antitumor effects, *Cancer Res.*, 2003, **63**, 8890–8898.
- 69 G. R. Macpherson, *et al.*, Anti-angiogenic activity of human endostatin is HIF-1-independent in vitro and sensitive to timing of treatment in a human saphenous vein assay, *Mol. Cancer Ther.*, 2003, **2**, 845–854.
- 70 V. P. Montecinos, *et al.*, Primary xenografts of human prostate tissue as a model to study angiogenesis induced by reactive stroma, *PLoS One*, 2012, **7**, e29623.